Journal of the Korea Concrete Institute
Vol.16 No.3, pp.441~450, June, 2004

Predictions of Seismic Behavior of Reinforced Concrete Bridge Columns

Tae-Hoon Kim[1)*], Woon-Hak Kim[2)], Kwang-Myong Lee[1)], and Hyun-Mock Shin[1)]

[1)]*Dept. of Civil and Environmental Engineering, Sungkyunkwan University, Korea*
[2)]*Dept. of Civil Engineering, Hankyong National University, Korea*

(Received January 30, 2004 ; Accepted April 15, 2004)

Abstract

The objectives of this study are to investigate the seismic behavior of reinforced concrete bridge columns and to provide the data for developing improved seismic design criteria. The accuracy and objectivity of the assessment process can be enhanced by the use of sophisticated nonlinear finite element analysis program. A computer program, named RCAHEST (Reinforced Concrete Analysis in Higher Evaluation System Technology), for the analysis of reinforced concrete structures was used. Material nonlinearity is taken into account by comprising tensile, compressive and shear models of cracked concrete and a model of reinforcing steel. The low-cycle fatigue damage of both concrete and reinforcing bars has been also considered in order to predict a reliable seismic behavior. The proposed numerical method for the prediction of seismic behavior of reinforced concrete bridge columns is verified by comparison with the reliable experimental results.

Keywords* : *seismic behavior, reinforced concrete bridge columns, material nonlinearity, low-cycle fatigue

1. Introduction

It is clear that a great majority of existing bridges in seismically active regions are vulnerable during earthquake. Therefore, more research is needed to expand knowledge on seismic behavior and design of bridge structures.

As a result of the damage that occurred to reinforced concrete bridge columns in recent earthquakes, major efforts were directed at developing strengthening or retrofit strategies to upgrade the seismic performance of reinforced concrete bridge columns.

Since only a limited number of large-scale experiments can be conducted due to the extensive cost and time commitment involved, the use of analytical models is necessary to better evaluate the performance of reinforced concrete bridge columns.[1,2)]

The evaluation of nonlinear hysteretic response of reinforced concrete structures under cyclic excitations requires the accurate and computationally efficient models of components and constituent materials.

Cyclic loading has a significant effect on the response, damage sequence, and failure mode of reinforced concrete bridge columns. The cyclic nature and severity of the seismic loading may require techniques to model the structural response and performance. Many parameters can influence the inelastic cyclic behavior of a reinforced concrete bridge column. Despite extensive research in understanding the cyclic material properties of reinforced concrete, its behavior is still not well established.[3-6)]

The main objective of this study is to characterize the seismic behavior of reinforced concrete bridge columns for seismic assessment and retrofit design. This paper describes the concrete and steel material models presently used in analytical procedures.

An evaluation method for seismic behavior of reinforced concrete bridge columns is proposed with using a nonlinear finite element program (RCAHEST, Reinforced Concrete Analysis in Higher Evaluation System Technology), developed in this study. The low-cycle fatigue model of concrete and that of reinforcing bars under cyclic load are newly incorporated into the material model for RCAHEST in order to predict the seismic behavior of reinforced concrete bridge columns.

* *Corresponding author*
Tel.: +82-31-290-7543; Fax.: +82-31-290-7549
E-mail address: neopilot@skku.edu

2. Nonlinear finite element analysis program

For the inelastic finite element analyses of reinforced concrete bridge columns under earthquake, a reinforced concrete plane stress element and an interface element have been developed.[1,2,7] The material models described in the next sections are used as the stress-strain relations at gauss integration points of each element. The formulation of elements requires coordinate transformation from the element coordinate system to the reference coordinate system.

The proposed structural element library RCAHEST (Reinforced Concrete Analysis in Higher Evaluation System Technology) is built around the finite element analysis program shell named FEAP, developed by Taylor.[8] FEAP is characterized by modular architecture and by the facility of introducing type of custom elements, input utilities and custom strategies and procedures.

Accompanying with the present study, authors attempt to implement such reinforced concrete plane stress element and interface element, and modify the material models in order to be suited to the fatigue damage analysis.

3. Nonlinear material model for RCAHEST

The nonlinear material model for the reinforced concrete is composed of models to characterize the behavior of the concrete, in addition to a model for characterizing the reinforcing bars. Models for concrete may be divided into models for uncracked concrete and cracked concrete. The basic model adopted for crack representation is a non-orthogonal fixed-crack method of the smeared crack concept, which is widely known to be a robust model for crack representation.

A full description of the nonlinear material model for reinforced concrete is given by Kim et al.[1,9] This section includes summary of the material models used in the analysis.

3.1 Model for uncracked and cracked concrete

The elasto-plastic and fracture model for the biaxial state of stress proposed by Maekawa and Okamura[10] is used as the constitutive equation for uncracked concrete.

After concrete cracks, the behavior becomes anisotropic in the crack direction. The stress-strain relations are modeled by being decomposed in directions parallel to, along and normal to cracks, respectively. Thus, the constitutive law adopted for the cracked concrete consists of tension stiffness, compression and shear transfer models. To obtain a more accurate tension stiffness model, the tensile stresses of concrete are transformed into the components in the direction normal to the crack. A modified elasto-plastic fracture model is used to describe the behavior of concrete in the direction of the crack plane. The model describes the degradation in compressive stiffness by modifying the fracture parameter in terms of the strain perpendicular to the crack plane. The shear transfer model based on the Contact Surface Density Function[11] is used to consider the effect of shear stress transfer due to the aggregate interlock at the crack surface.

3.2 Model for the reinforcing bars in concrete

The constitutive equations for the bare bar may be used if the stress-strain relation remains in the elastic range. The post-yield constitutive law for the reinforcing bar in concrete considers the bond characteristics and the model is a bilinear model.

The transverse reinforcements confine the compressed concrete in the core region and inhibit the buckling of the longitudinal reinforcing bars. In addition, the reinforcements also improve the ductility capacity of the unconfined concrete. This study adopted a model proposed by Mander et al.[12]

3.3 Model and assumption for the interface

According as stiffness changes rapidly on column and foundation, the local discontinuous deformation happens as part of anchorage slip, shear slip, and penetration at joint plane. Therefore, the interface element is required to obtain more accurate prediction of response of structures at the boundary plane.[1]

The interface model for the boundary plane connecting two reinforced concrete elements with different sections is based on the discrete crack concept, which uses the relationships between the stresses and the localized deformations. The model is one-dimensional and has no thickness.[1]

4. Material model's correction to consider fatigue damage

Fatigue damage of reinforced concrete bridge columns under cyclic load such as seismic load appears necessarily. Fatigue damage influencing inelastic behavior of reinforced concrete bridge column, may be divided into concrete strength deterioration and low-cycle fatigue of reinforcing bars. This study considers above effects through nonlinear material model's correction and so on.

4.1 Fatigue model of reinforcing bars

Reinforcing bars dominate behavior of reinforced concrete members subjected to seismic load. Low-cycle fatigue

by load reversals is notable form of failure in bending member.[13]

It was proved that plastic strain of reinforcing bars is important variable of low-cycle fatigue from several researches. This study applied Coffin–Manson's equation[14] as follows.

$$\varepsilon_{ap} = 0.0777(N_{2fo})^{-0.486} \quad (1)$$

where, $\varepsilon_{ap} = \frac{\Delta\varepsilon_p}{2}$; $\Delta\varepsilon_p = (\varepsilon_p)_{\max} - (\varepsilon_p)_{\min}$; N_{2fo} = number of complete cycles to failure for original model; $(\varepsilon_p)_{\max}$ = maximum strain by number of cycles; and $(\varepsilon_p)_{\min}$ = minimum strain by number of cycles.

In spite of reliability of Eq. (1), the N_{2fo} needs to be modified to apply to the reinforced concrete, because Eq. (1) was derived from the bare bar test. From the results of the parametric study in the next section, the N_{2fo} is yielded the following relationship.

$$N_{2fr} = k_r N_{2fo} \quad (2)$$

where, N_{2fr} = number of complete cycles to failure for reinforcing bars; k_r = modification factor for reinforcing bars determined from the parametric study in the next section (= $\alpha_1 s_k$); $s_k = \frac{f'_{cc}}{f'_{co}}$; f'_{cc} = confined concrete compressive strength; and f'_{co} = unconfined concrete compressive strength.

Following Miner's rule,[15] the accumulated fatigue damage of reinforcing bars (AD_r) can be derived.

$$AD_r = \sum_1^n \frac{1}{(N_{2fr})_i} \quad (3)$$

4.2 Fatigue model of concrete

One of the important characteristics of the fatigue process is the strength degradation under cyclic loading. Experimental results show that the degradation is a function of the number of load repetitions, as well as the maximum and minimum stresses of the load cycles.

Kakuta et al.'s formula[16] derived from plain concrete specimens tests is adopted for fatigue model of concrete basically.

The modifications are adopted to apply to the reinforced concrete. One is to determine the number of cycles to failure by strains in calculated gauss integral calculus point instead of by stress in Kakuta et al.'s formula, and the other is to multiply a modification factor to apply to the reinforced concrete like as fatigue model of reinforcing bars.

$$\log\frac{N_{2fc}}{k_c} = \begin{cases} \frac{1}{\beta}\left[1 - \frac{(\varepsilon_{co} - \varepsilon_{\min})^2 - (\varepsilon_{co} - \varepsilon_{\max})^2}{(\varepsilon_{co} - \varepsilon_{\min})^2}\right], & \varepsilon_{\max} < 0.7\varepsilon_{co} \\ \frac{0.09\varepsilon_{cu}}{\varepsilon_{cu} - 0.7\varepsilon_{co}} \frac{1}{\beta} \frac{\varepsilon_{\max} - \varepsilon_{\min}}{\varepsilon_{cu} - \varepsilon_{\min}}, & \varepsilon_{\max} \geq 0.7\varepsilon_{co} \end{cases} \quad (4)$$

where, N_{2fc} = number of complete cycles to failure for concrete; ε_{co} = strain of unconfined concrete at peak stress; $\varepsilon_{\min}$ = cyclic minimum strain; $\varepsilon_{\max}$ = cyclic maximum strain; ε_{cu} = compressive strain of confined concrete at failure; β = material constant equal to 0.0588; and k_c = modification factor for concrete determined from the parametric study in the next section (= $\alpha_2 s_k$).

Miner's rule is also considered concrete fatigue damage.

4.3 Parametric study for modification factor

4.3.1 Description of low-cycle fatigue tests

The Low-cycle fatigue tests performed at the University of Central Florida.[17-19] These tests provided the basis for developing a fatigue-life expression for the specimen.

Table 1 lists the dimensions, reinforcement details, applied axial load and lateral load capacity for both the prototype and the model. Dimensional and reinforcement details of the specimen are shown in Fig. 1. Details of material properties can be found in Table 2.

Specimen A3 was subjected to constant 2 percent lateral drift amplitude cycles until failure. Specimen A4 was subjected to repeated cyclic loading at a constant displacement amplitude of ± 57 mm until failure. This displacement was equal to a drift of approximately 4.0 percent. Specimen A5 was tested under repeated cyclic loading at a constant displacement amplitude of ± 75 mm, corresponding to a drift of approximately 5.5 percent. The final Specimen (A6) to be tested under constant amplitude loading was subjected to a displacement amplitude of ± 95 mm, corresponding to approximately 7 percent drift.

4.3.2 Numerical simulation for modification factor determination

Fig. 2 shows the finite element discretization and the boundary conditions for seismic analyses of the reinforced concrete bridge columns. The interface element between the footing and the column enhance the effects of the bond-slip of steel bars and the local compression.

Table 1 Details of prototype and model

Item	Prototype	Model	Remarks
Longitudinal reinforcement	24 No. 11 (36 mm)	21 No. 3 (9.5 mm)	ρ = 2 %
Spirals	No. 5 (16 mm)	Wire = 4 mm diameter	Smooth wire
Spirals pitch	76 mm	19 mm	ρ_v = 1 %
Spiral yield strength	414 MPa	380 to 450 MPa	-
Column diameter	1.22 m	0.3 m	Scale 1:4
Column length	5.5 m	1.37 m	Scale 1:4
Cover	50 mm	12.5 mm	Scale 1:4
Embedment length of bars	Tension = 1.4 m Compression = 0.72 m	Tension = 0.35 m Compression = 0.18 m	-
Axial load	3225 kN	806 kN	$0.1 f_c' A_g$
Lateral load capacity	1550 kN	388 kN	$V_p = M_p / H$
Spacing of longitudinal steel	100 mm	25 mm	-

Table 2 Material characteristics

Specimen	Concrete strength (MPa)	Steel yield strength (MPa)	Spiral yield strength (MPa)
A2 – A3	29	448	434
A4 – A6	35.5	448	434
A7 – A8	32.8	448	434
A9	32.5	448	434
A10 – A12	27.0	448	434

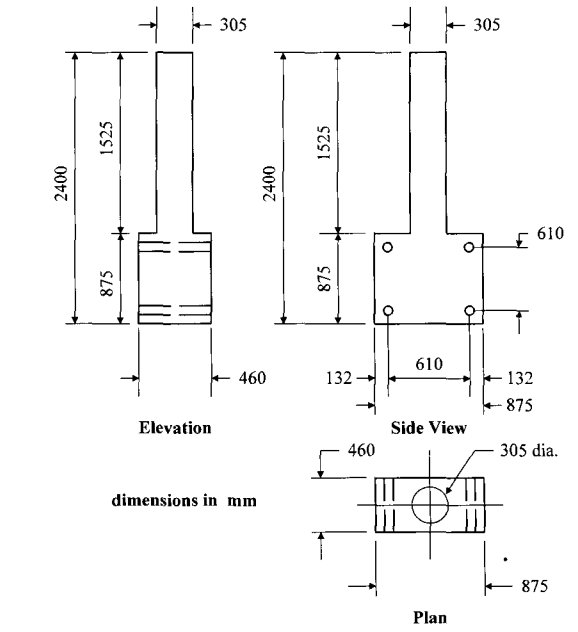

(a) Configuration and dimensions

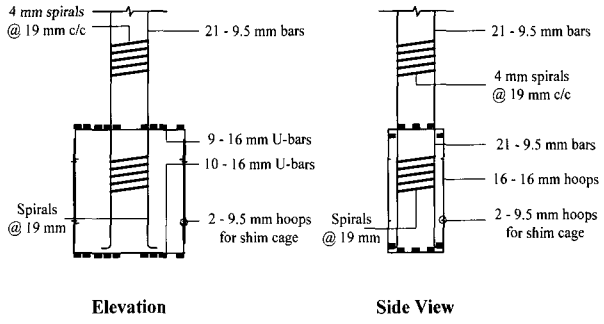

(b) Reinforcement arrangement

Fig. 1 Specimen details

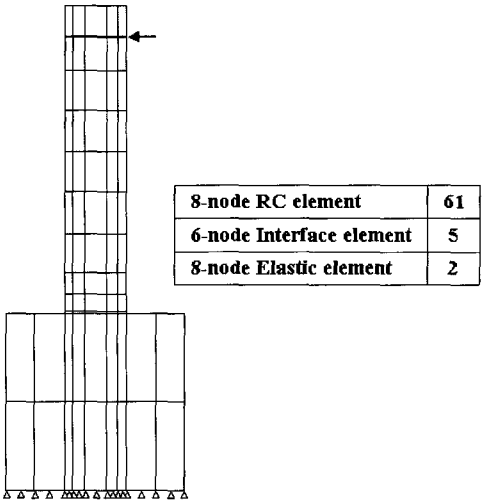

Fig. 2 Finite element mesh for analysis

Fig. 3 shows a method for transforming a circular section into rectangular strips for using plane stress elements. For rectangular sections, equivalent strips are calculated. After the internal forces are calculated, the equilibrium is checked. Loading cycles with displacement control are applied as this allows the analysis beyond the ultimate load where the load at the maximum strain is recognized from the load displacement curve.

Table 3 shows the effect of modification factor $k_r (=\alpha_1 s_k)$ and $k_c (=\alpha_2 s_k)$ on the ultimate shear strength degradation. Figure 4 also shows the strength gradient for twelve situations at five different cycle numbers. Modification factors are varied from $1.0\,s_k$ to $2.5\,s_k$ with increasing normalized cycle number.

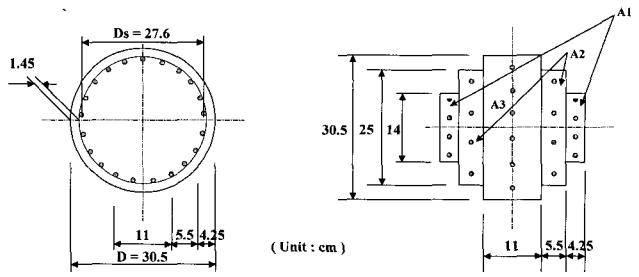

Fig. 3 Transformation of a circular column to an idealized equivalent rectangular column

From the results of the numerical tests, the $\alpha_1 = 1.5$ and $\alpha_2 = 2.0$ are yielded. The results were found to have a mean of 1.00 and a coefficient of variation (COV) of 17%. The assumptions given above are supported by sound engineering judgment, and the good agreement obtained between analyses and experiments.

4.3.3 Comparison with benchmark tests

Benchmark experiments have been simulated with this model to verify its accuracy. These benchmark tests included characterization of the fatigue behavior of the model bridge columns.

Fig. 5 shows good agreement between the experimental results and the numerical ones, for the standard cyclic test (A2). Specimen A2 was subjected to three cycles each at lateral displacement amplitudes of 1.0, 1.5, 2.0, 2.5, 3.0, 4.0,plitude testing. The figure compares the analysis results for the cases with and without the fatigue model. The hysteresis is stable until 6.0% drift in the analysis without fatigue model, while the restoring force significantly deteriorates at 6.0% drift in the analysis with fatigue model. Agreements are satisfactory. Stiffness at unloading and reloading paths from the peak displacements gradually deteriorates as the displacement increases. It is noted that the degradation observed experimentally with repeated loading to the same ductility level could also be captured with the adopted set of material models.

5. Numerical examples

From numerical analysis of the tested specimens, it is found that the proposed numerical method is sufficiently accurate for the analysis of reinforced concrete bridge columns.

5.1 Specimens and analytical model description

The proposed numerical method is applied to reinforced concrete bridge columns subjected to different types of loading.[17-19]

Table 3 Experiment and analysis results by modification factor

Item		(1) Ana. /Exp. $\alpha_1=1.0$ $\alpha_2=1.0$	(2) Ana. /Exp. $\alpha_1=1.5$ $\alpha_2=1.0$	(3) Ana. /Exp. $\alpha_1=2.0$ $\alpha_2=1.0$	(4) Ana. /Exp. $\alpha_1=1.0$ $\alpha_2=1.5$	(5) Ana. /Exp. $\alpha_1=1.5$ $\alpha_2=1.5$	(6) Ana. /Exp. $\alpha_1=2.0$ $\alpha_2=1.5$	(7) Ana. /Exp. $\alpha_1=1.0$ $\alpha_2=2.0$	(8) Ana. /Exp. $\alpha_1=1.5$ $\alpha_2=2.0$	(9) Ana. /Exp. $\alpha_1=2.0$ $\alpha_2=2.0$	(10) Ana. /Exp. $\alpha_1=1.0$ $\alpha_2=2.5$	(11) Ana. /Exp. $\alpha_1=1.5$ $\alpha_2=2.5$	(12) Ana. /Exp. $\alpha_1=2.0$ $\alpha_2=2.5$
A3	0.4	0.96	0.96	0.96	0.95	0.96	0.96	0.96	0.96	0.95	0.95	0.96	0.96
	0.6	0.96	0.97	0.98	0.98	0.99	0.99	0.99	0.99	0.99	0.98	0.99	0.99
	0.8	0.91	0.92	0.95	0.95	0.95	0.93	0.92	0.95	0.95	0.94	0.95	0.95
	1.0	0.87	0.90	0.95	0.96	0.98	0.95	0.93	0.98	0.98	0.96	0.98	0.98
A4	0.4	1.05	1.07	1.07	1.05	1.07	1.08	1.06	1.06	1.07	1.05	1.06	1.07
	0.6	0.92	1.03	1.03	0.98	1.04	1.09	1.00	1.05	1.08	0.98	1.06	1.09
	0.8	0.92	0.96	0.97	0.95	1.05	1.14	1.00	1.07	1.15	1.01	1.11	1.14
	1.0	0.95	0.97	0.93	0.91	1.07	1.11	1.00	1.06	1.20	1.02	1.10	1.20
A5	0.4	0.99	0.97	0.99	0.98	0.97	0.99	0.95	0.98	0.99	0.97	0.98	0.97
	0.6	0.91	0.95	1.01	0.93	0.97	1.01	0.83	0.97	1.01	0.99	0.97	0.97
	0.8	0.82	0.86	0.95	0.85	0.93	0.96	0.76	0.93	0.96	0.83	0.94	0.89
	1.0	0.66	0.51	0.72	0.69	0.70	0.75	0.36	0.70	0.75	0.68	0.71	0.60
A6	0.4	0.92	0.83	0.87	0.83	0.84	0.88	0.83	0.83	0.87	0.83	0.84	0.94
	0.6	0.92	0.92	0.89	0.92	0.94	0.94	0.87	0.91	0.93	0.86	0.94	0.95
	0.8	1.00	1.01	1.00	0.93	1.02	1.03	0.96	1.02	1.01	0.95	1.04	1.04
	1.0	1.45	1.50	1.53	1.47	1.51	1.54	1.48	1.52	1.64	1.48	1.54	1.56
Mean		0.95	0.96	0.99	0.96	1.00	1.02	0.93	1.00	1.03	0.97	1.01	1.02
COV		0.17	0.20	0.17	0.17	0.17	0.17	0.23	0.17	0.19	0.17	0.17	0.19

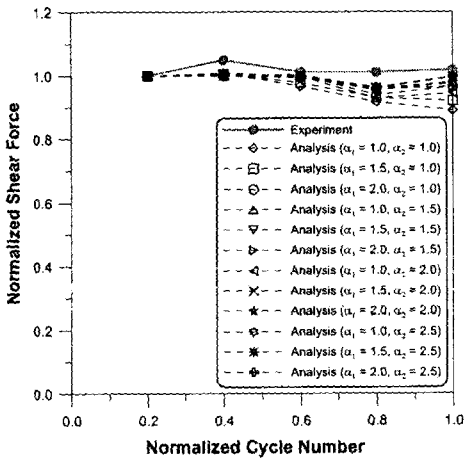

(a) A3

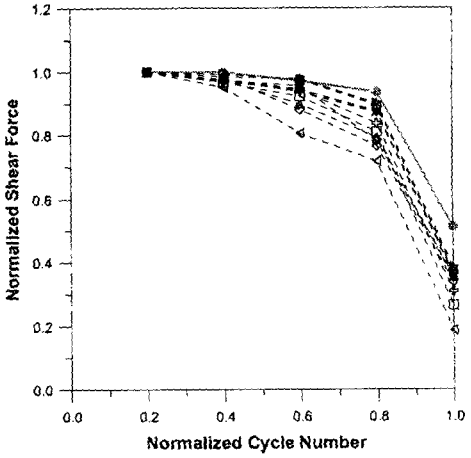

(c) A5

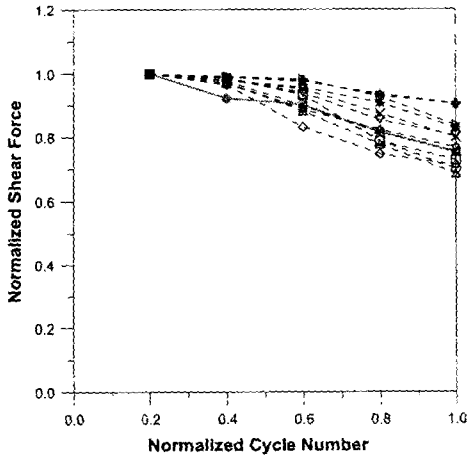

(b) A4

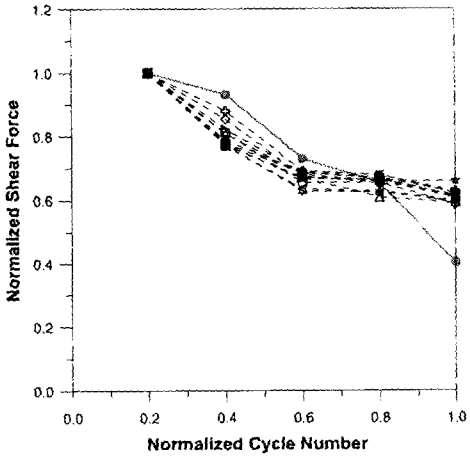

(d) A6

Fig. 4 Normalized shear force vs. normalized cycle number

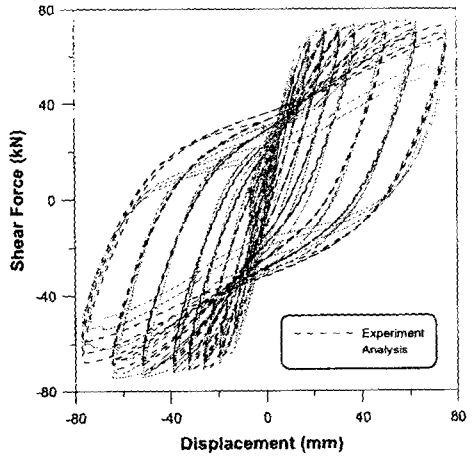

(a) Analysis without fatigue model

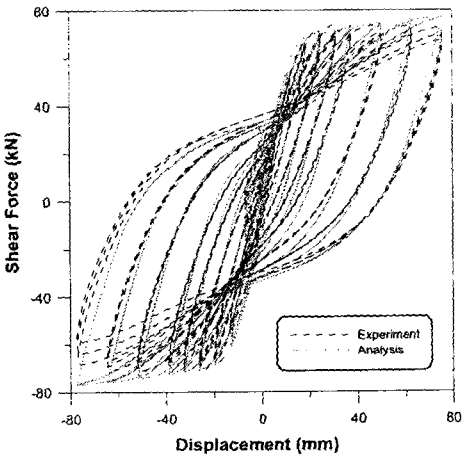

(b) Analysis with fatigue model

Fig. 5 Shear force vs. displacement hysteresis (A2)

The experimental program consisted of tests on quarter-scale, circular, reinforced concrete bridge columns. The test specimens were subjected to random displacement histories as shown in Table 4. The imposed displacement histories were obtained from analytical simulations of the model column subjected to a sequence of earthquakes of varying duration and magnitude.

Analytical model descriptions are presented in the previous section, additional verification with variable amplitude tests is presented in this section. This description is intended to allow the reader to simulate the experiments, provided proper numerical models are available.

5.2 Comparison with experimental results

Specimen A7 was subjected to variable amplitude displacement cycles generated from four different earthquakes. The total displacement history imposed on specimen A8 was essentially the same as that used in specimen A7, but the sequence of events was changed (Table 4). Specimens A9 and A10 were subjected to a different set of load reversals resulting from a different sequence of events (Table 4). The largest amplitudes were imposed by earthquake No. 1 on specimen A11, which failed midway through earthquake No. 4. For specimen A12, the largest amplitudes were

Table 4 Ground motions selected for generating random displacement histories for specimens A7 to A12

Specimen	Event	Description	Purpose	Record	Scale	PGA, g
A7	1	Damaging earthquake	First major event	Loma Prieta 1989 Presidio	12.00	1.20
	2	Minor earthquake	Aftershock	Imperial Valley 1979 Superstition Mt.	1.80	0.34
	3	Minor earthquake	Second aftershock	San Fernando 1971 2011 Zonal Ave.	1.20	0.10
	4	Severe earthquake	Failure of bridge	San Fernando 1971 455 S. Figueroa St.	3.60	0.54
A8	1	Minor earthquake	Minor damage	Imperial Valley 1979 Superstition Mt.	1.80	0.34
	2	Minor earthquake	Additional damage	San Fernando 1971 2011 Zonal Ave.	1.20	0.10
	3	Damaging earthquake	First major event	Loma Prieta 1989 Presidio	12.00	1.20
	4	Severe earthquake	Failure of bridge	San Fernando 1971 455 S. Figueroa St.	3.60	0.54
A9	1	Major earthquake	First major event	San Fernando 1971 Orion Blvd.	3.25	1.43
	2	Minor earthquake	Aftershock damage	San Fernando 1971 2011 Zonal Ave.	1.20	0.10
	3	Moderate earthquake	Additional damage	El Centro 1940	1.00	0.35
	4	Minor earthquake	Aftershock	San Fernando 1971 455 S. Figueroa St.	1.00	0.15
	5	Severe earthquake	Failure of structure	San Fernando 1971 Orion Blvd.	3.25	1.43
A10	1	Minor earthquake	Minor damage	San Fernando 1971 2011 Zonal Ave.	1.20	0.10
	2	Moderate earthquake	Additional damage	El Centro 1940	1.00	0.35
	3	Minor earthquake	Aftershock	San Fernando 1971 455 S. Figueroa St.	1.00	0.15
	4	Major earthquake	First major event	San Fernando 1971 Orion Blvd.	3.25	1.43
	5	Severe earthquake	Failure of structure	San Fernando 1971 Orion Blvd.	3.25	1.43
A11	1	Major earthquake	First damaging earthquake	Northridge 1994 VA Hospital	1.00	0.42
	2	Minor earthquake	Aftershock	Northridge 1994 Griffith Observatory	1.00	0.26
	3	Minor earthquake	Additional damage	Taft 1952	1.00	0.36
	4	Severe earthquake	Failure of column SCT	Mexico City 1985	1.00	0.17
A12	1	Minor earthquake	Minor damage	Northridge 1994 Griffith Observatory	1.00	0.26
	2	Minor earthquake	Additional damage	Taft 1952	1.00	0.36
	3	Major earthquake	First damaging earthquake	Northridge 1994 VA Hospital	1.00	0.42
	4	Severe earthquake	Failure of column SCT	Mexico City 1985	1.00	0.17

reserved for the final cycles. The objective in this series of testing was to induce fatigue failure of the longitudinal bars, and hence the events were selected to produce significantly larger displacement amplitudes.

Figs. 6 through 11 compare the analytical shear vs. displacement responses with the experimental results. The analytical results show good agreement with the experimental results. Each figure also compares the analysis results with and without the fatigue model. The shear hysteretic response is well represented by the analytical model. Figures indicate that the analytical model adequately captures the column stiffnesses at yield and just after the initiation of shear failure, and correctly detects the cycles in which the column shear strength degradation begins.

Seismic behavior prediction by proposed numerical method can evaluate well damage or failure of each load step generally from these results. In conclusion, it was necessary to form a mathematical model that could simulate the behavior of such structures with reasonable accuracy when compared with test results.

6. Conclusions

A nonlinear finite element program, RCAHEST, developed to compute inelastic response of reinforced concrete bridge columns subjected to a variety of types of loading, produces good correlation with experimental data. The low-cycle fatigue damage of both concrete and reinforcing bars has been taken into account to predict a reliable seismic behavior.

A comparison with test data confirms that good predictions were obtained in regards to load capacities, failure modes, and load-deformation responses of reinforced concrete bridge columns. It is concluded that the proposed numerical method is a reasonable combination between ductility and low-cycle fatigue damage and it gives good results compared to the observed behavior for tests.

More efforts should be directed to include certain procedures in the current design codes to direct the engineers toward an acceptable method for evaluating the available strength in existing reinforced concrete bridge columns.

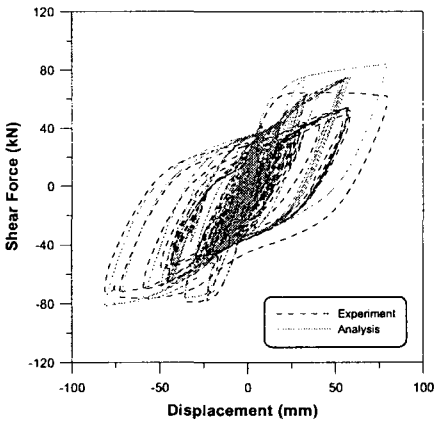

(a) Analysis without fatigue model

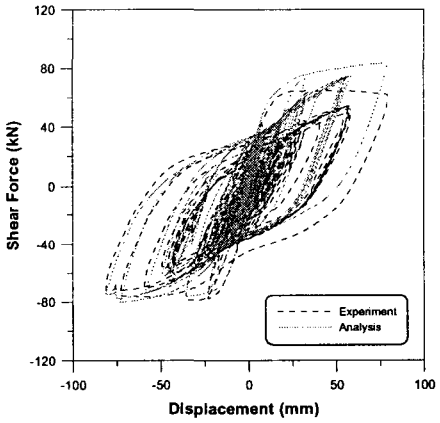

(b) Analysis with fatigue model

Fig. 6 Shear vs. displacement response for specimen A7

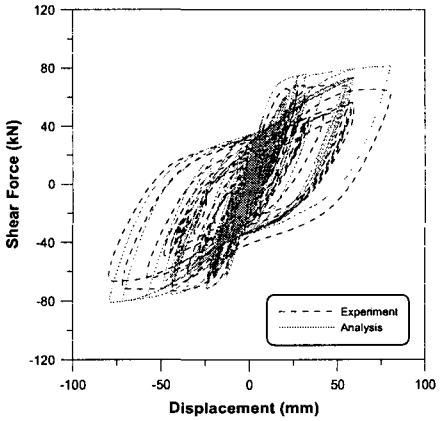

(a) Analysis without fatigue model

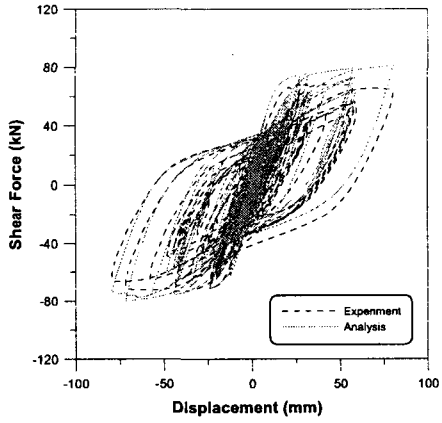

(b) Analysis with fatigue model

Fig. 7 Shear vs. displacement response for specimen A8

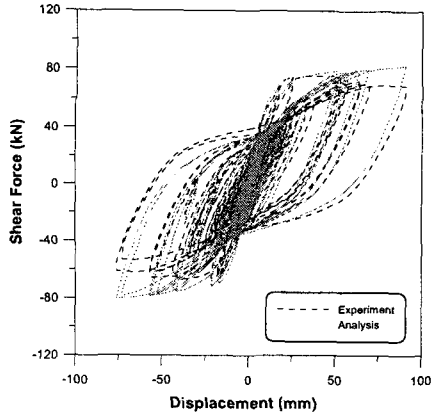

(a) Analysis without fatigue model

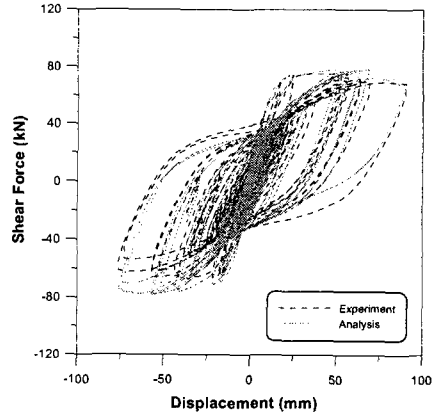

(b) Analysis with fatigue model

Fig. 8 Shear vs. displacement response for specimen A9

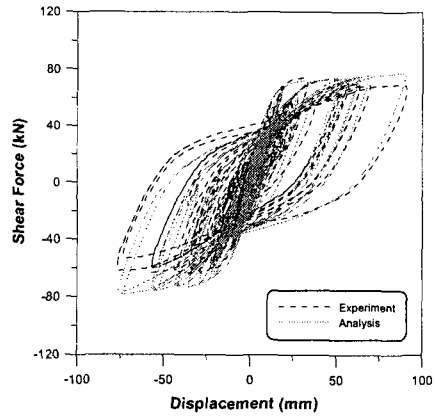

(a) Analysis without fatigue model

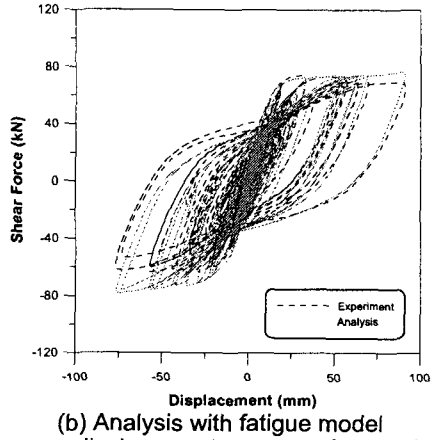

(b) Analysis with fatigue model

Fig. 9 Shear vs. displacement response for specimen A10

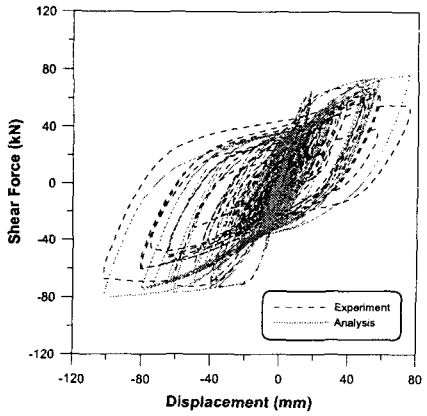

(a) Analysis without fatigue model

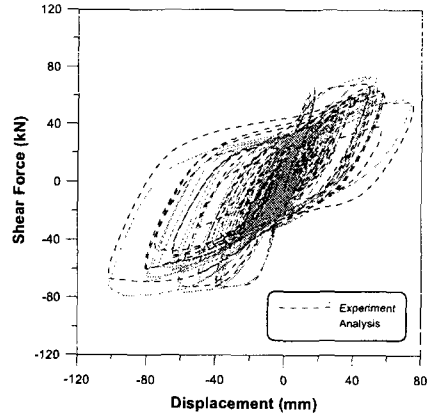

(b) Analysis with fatigue model

Fig. 10 Shear vs. displacement response for specimen A11

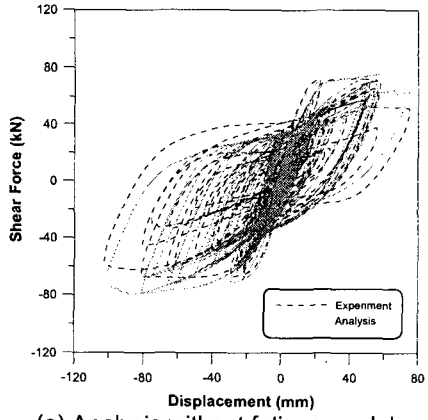

(a) Analysis without fatigue model

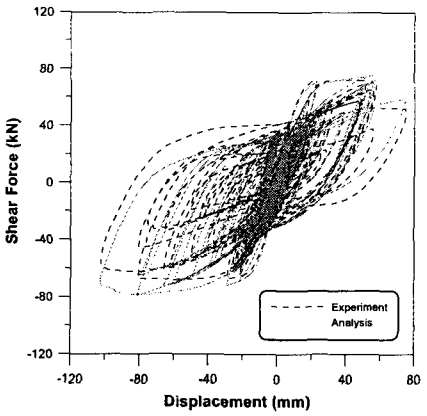

(b) Analysis with fatigue model

Fig. 11 Shear vs. displacement response for specimen A12

Acknowledgements

The study described in this paper was supported by the Korea Science and Engineering Foundation (KOSEF) through the Korea Earthquake Engineering Research Center (KEERC). The authors wish to express their gratitude for the support received.

References

1. Kim, T. H., Lee, K. M., Yoon, C. Y., and Shin, H. M., 2002b, "Inelastic Behavior and Ductility Capacity of Reinforced Concrete Bridge Piers under Earthquake. Ⅰ: Theory and Formulation," *Journal of Structural Engineering*, ASCE, Vol.129, No.9, 2003, pp.1199~1207.
2. Kim, T. H., Lee, K. M., Yoon, C. Y., and Shin, H. M., "Inelastic Behavior and Ductility Capacity of Reinforced Concrete Bridge Piers under Earthquake. Ⅱ: Numerical Validation," *Journal of Structural Engineering*, ASCE, Vol.129, No.9, 2003, pp.1208~1219.
3. Pincheira, J. A., Ditwala, F. S., and D'Souza, J. T., "*Seismic Analysis of Older Reinforced Concrete Columns*," Earthquake Spectra, Vol.15, No.2, 1999, pp.245~272.
4. Yalcin, C. and Saatcioglu, M., "Inelastic Analysis of Reinforced Concrete Columns," *Computer and Structures*, Vol. 77, 2000, pp.539~555.
5. Lee, D. H. and Elnashai, A. S., "Seismic Analysis of RC Bridge Columns with Flexure-Shear Interaction," *Journal of Structural Engineering*, ASCE, Vol.127, No.5, 2001, pp. 546~553.
6. Kwan, W.-P. and Billington, S. L., "Simulation of Structural Concrete under Cyclic Load," *Journal of Structural Engineering*, ASCE, Vol.127, No.12, 2001, pp.1391~1401.
7. Kim, T. H. and Shin, H. M., "Analytical Approach to Evaluate the Inelastic Behaviors of Reinforced Concrete Structures under Seismic Loads," *Journal of the Earthquake Engineering Society of Korea*, EESK, Vol.5, No.2, 2001, pp. 113~124.
8. Taylor, R. L., "*FEAP - A Finite Element Analysis Program*," Version 7.2 Users Manual," Vol.1 & Vol.2, 2000.
9. Kim, T. H., Lee, K. M., and Shin, H. M., "Nonlinear Analysis of Reinforced Concrete Shells using Layered Elements with Drilling Degree of Freedom," *ACI Structural Journal*, Vol.99, No.4, 2002, pp.418~426.
10. Maekawa, K. and Okamura, H., "The Deformational Behavior and Constitutive Equation of Concrete Using Elasto-Plastic and Fracture Model," *Journal of the Faculty of Engineering*, University of Tokyo, Vol.37, No.2, 1983, pp.253~328.
11. Li, B. and Maekawa, K., "Contact Density Model for Stress Transfer across Cracks in Concrete," *Concrete Engineering*, JCI, Vol.26, No.1, 1988, pp.123~137.
12. Mander, J. B., Priestley, M. J. N., and Park, R., "Theoretical Stress-Strain Model for Confined Concrete," *Journal of Structural Engineering*, ASCE, Vol.114, No.8, 1988, pp.1804~1826.
13. Perera, R., Carnicero, A., Alarcon, E., and Gomez, S., "A Fatigue Damage Model for Seismic Response of RC Structures," *Computer and Structures*, Vol.78, 2000, pp. 293~302.
14. Mander, J. B., Panthaki, F. D., and Kasalanati, K., "Low-Cycle Fatigue Behavior of Reinforcing Steel," *Journal of Materials in Civil Engineering*, ASCE, Vol.6, No.4, 1994, pp. 453~468.
15. Miner, M. A., "Cumulative Damage in Fatigue," *Journal of Applied Mechanics*, Vol. 67, 1945, pp. A159~A164.
16. Kakuta, Y., Okamura, H., and Kohno, M., "New Concepts for Concrete Fatigue Design Procedures in Japan," *IABSE Colloquium of Fatigue of Steel and Concrete Structures*, Lausanne, 1982, pp.51~58.
17. Kunnath, S. K., El-Bahy, A., Taylor, A. W., and Stone, W. C., "*Cumulative Seismic Damage of Reinforced Concrete Bridge Piers*," Report No. NCEER-97-0006, National Center for Earthquake Engineering Research, State University of New York at Buffalo. 1997.
18. El-Bahy, A., Kunnath, S. K., Stone, W. C., and Taylor, A. W., "Cumulative Seismic Damage of Circular Bridge Columns: Benchmark and Low-Cycle Fatigue Tests," *ACI Structural Journal*, Vol.96, No.4, 1999, pp.633~641.
19. El-Bahy, A., Kunnath, S. K., Stone, W. C., and Taylor, A. W., "Cumulative Seismic Damage of Circular Bridge Columns: Variable Amplitude Tests," *ACI Structural Journal*, Vol.96, No.5, 1999, pp.711~719.